Tracking and Data Fusion in a Passive Radar System

D. Fränken, S. Stroth, O. Zeeb
HENSOLDT Sensors GmbH
Woerthstrasse 85, 89077 Ulm
GERMANY

oliver.zeeb@hensoldt.net

ABSTRACT

Passive radar (PR) systems rely on third-party transmitters like, e.g., analog or digital audio or video broadcasting stations to illuminate targets of interest. Lacking own emitting sources, these systems are fairly lightweight and mobile. They can be set up at arbitrary locations including densely populated areas, and inherently they possess advantageous stealth properties. The creation of an overall target situation picture is based on the evaluation of both the reflections from the target and the transmitted signals received directly from the illuminating transmitters. Signal processing delivers plots with bistatic range, Doppler and favourably azimuth and elevation, depending on the applied antenna technology. Tracking and data fusion are subsequently applied to create the situation picture. This paper discusses tracking and data fusion in an integrated FM/DAB/DVB-T PR system for airspace surveillance tasks and presents typical effects in passive radar systems that are not familiar from classical monostatic radar tracking.

1 BISTATIC DATA

In classical monostatic radar systems, the emitter and receiver of a signal are positioned at the same location. Passive radar systems, however, use signals of opportunity from fixed antennas in different locations. Thus, tracking in passive radar systems differs from classical radar systems. The geometry and the nature of the bistatic measurements, which are not Cartesian complete, imply several consequences [1, 2].

1.1 Passive Radar Tracking in General: From Bistatic to Cartesian Data.

In a classical Radar, the emission time of a signal is known, so the time until an echo is received defines the euclidian distance from the target to the radar sensor. Additional measurement of the azimuth and elevation make an observation cartesian complete, i.e. the 3D-location of the target is known. However, since passive radar systems rely on third-party transmitters, the signal emission time is unknown and bistatic plots comprise the Time-Difference-of-Arrival (TDoA), i.e., the time difference between the direct signal and the reflected signal. The TDoA can be converted into a bistatic range. Such a bistatic range measurement of a target defines an ellipsoid (or in 2D an ellipse) with the receiver and the transmitter as focal points and the target on the ellipse, see Figure 1 (red ellipse).

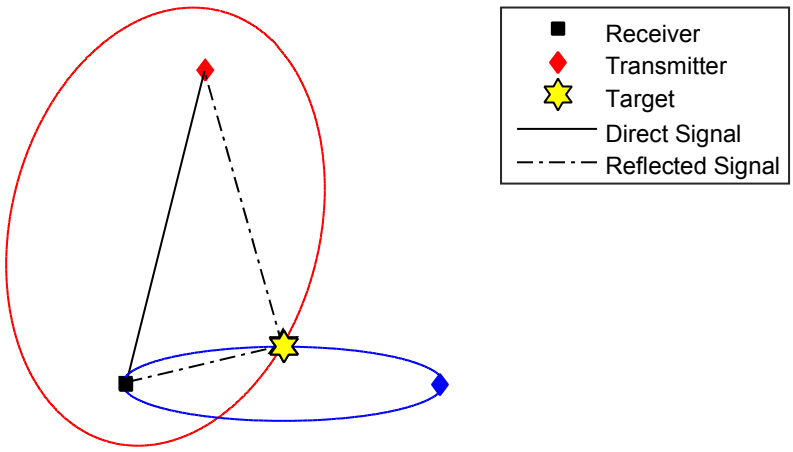

Figure 1: Bistatic geometry.

Without further information, the target that reflects the signal could be *anywhere* on the ellipse, the cartesian position can not be uniquely determined. If additionally the reflected signal from a second illuminator (blue) is measured, the intersection of these two ellipses defines possible target locations. Note, that still the target position is not uniquely determined since in general there are multiple intersection points, see again Figure 1: the true target location at the yellow marker and the additional intersection a bit below.

The addition of more target measurements originating from different illuminators, i.e., the intersection of n>2 ellipses, could define the target location uniquely as the single point which *all* ellipses have in common, see Figure 2.

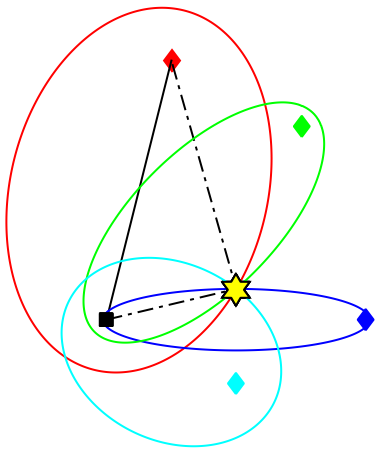

Figure 2: Intersection of n ellipses (n=4).

Since in reality the measurements naturally comprise measurement errors, the measured bistatic range does not represent the actual bistatic range exactly. This leads to the situation that a (desirable) common intersection point for all the ellipses does not exist. Instead there are several intersection points which are close to each other. Simple ellipse intersection algorithms for all the illuminators to detect the target location can therefore not be applied. Instead, mathematical tools dealing with uncertainties and probabilities have to be invoked. This situation is visualized in Figure 3 where the transparent belt around the ellipse sectors shall visualize the uncertainty.

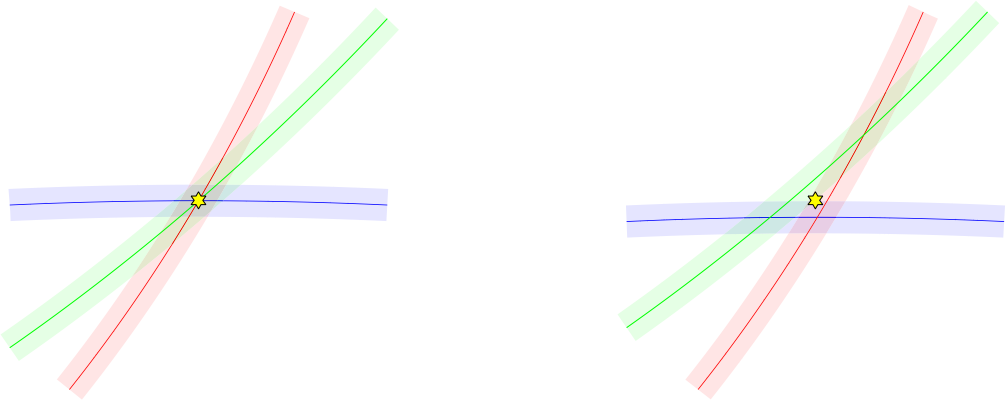

Figure 3: Intersection with ideal (left) and defective (right) measurements.

Invocation of more illuminators leads to more intersection points of the ellipses, see again Figure 2. These additional intersections can lead to so called “ghost targets”. That are tracks which appear in the final target situation picture but do not originate from true targets although they behave as such. These ghosts stem from faulty data association and should have been rejected during the tracking algorithms.

If in addition to the bistatic range-rate the azimuth is measured, ghosts can be identified as such more precisely. Figure 4 (left) visualizes this situation: The yellow intersection point represents the true target which is identified as such by the support of the azimuth estimation (grey cone) whereas the green intersection point can be identified as a ghost target and is excluded from further processing. A zoom of this situation in Figure 4 (right) also explains, why no direction finding algorithms [3] to detect the true target location can be applied. Such algorithms compute the intersection point of the ellipse with the measured azimuth angle. However, small uncertainties in the azimuth estimation - the azimuth accuracy of PR systems is usually much lower than in active radars - can lead to rather large location uncertainties. The bold red and blue sections of the ellipse symbolize possible target locations that result from a direction finding algorithm which takes the azimuth uncertainty into account. This figure also shows the geometry dependence of the passive radar system: The azimuth estimation supports the target location estimation to a much higher extent for the red illuminator than for the blue one. In reality, the azimuth angle can mainly be used for gating, i.e., a coarse choice of possible target locations and exclusion of ghost locations as mentioned above.

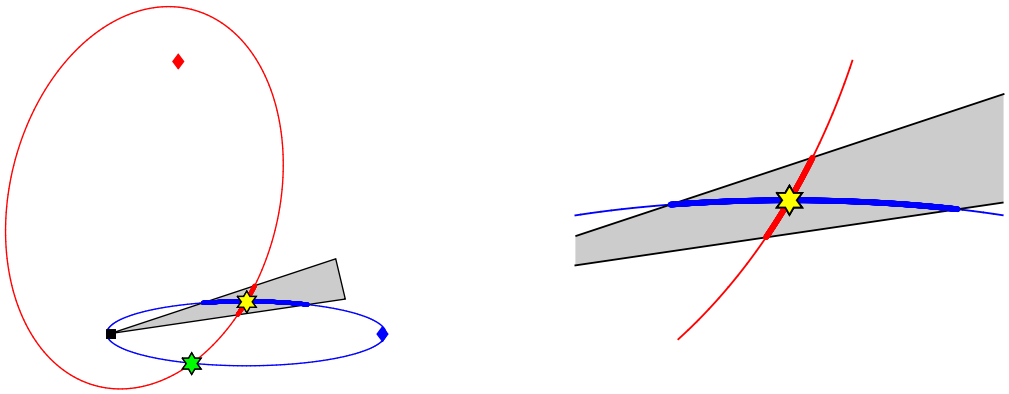

Figure 4: Azimuth estimation.

1.2 3-Stage-Tracking

Assume a scenario with one sensor and N illuminators in different geographical locations. In the ideal case, a target is detected by all of the N illuminator-sensor-combinations, i.e., in the signal processing one target generates N bistatic plots (i.e., N ellipses) at one instant of time. In order to obtain Cartesian tracks of targets, three stages are applied in the tracking and data fusion system (see also [4, 5, 6] and references therein):

1.) Bistatic Plots → Range-RangeRate-Tracks (R^3-Tracking)

2.) Range-RangeRate-Tracks → 3D-Tracks (Cartesian Tracking)

3.) Bistatic Plots → Cartesian Tracks (Feedback Loop)

After the creation of the bistatic Plots, in Stage 1 a bistatic tracking is performed in the measurement space for each illuminator separately, i.e., N tracks with bistatic range and range-rate are created. This helps to suppress clutter plots, as all the bistatic plots that do not support a Range-RangeRate-Track (R^3-Track) are identified as clutter and are not passed to the second stage.

As explained above, the information of a single R^3-Track is not sufficient to determine the Cartesian, i.e., 3D-position of a target. Therefore, the R^3-Tracks detected in Stage 1 are intersected with each other in Stage 2. This leads to Cartesian positions and velocities of a target. This stage is computationally very demanding because of the many possible combinations of different R^3-tracks from several illuminators (cf. the many intersection points of the ellipses in Figure 2).

In Stage 3, these Cartesian 3D-tracks are fed back into the tracking system in order to reduce the computational load. Once a 3D-Track has been initiated, this track has direct access to the bistatic measurements received from the signal processing, before they are passed to R^3-Tracking (i.e., before Stage 1). For this purpose, the 3D-Kinematic is transformed to a bistatic kinematic for each sensor-illuminator pair seperately and can then be compared with incoming bistatic plots. If a bistatic plot fits to the track, it is directly associated to it and this plot does not need to be processed further in Stage 1 or 2. With this feedback loop, the computational load of the overall tracking system is reduced significantly.

2 CHALLENGES IN BISTATIC TRACKING

As described above, many challenges in passive radar tracking arise from the bistatic geometry and the Cartesian incomplete nature of the measurements. Additionally, in classical radar systems, the underlying signals are known and can be controlled (e.g. wave form, frequency, emission time, ...). This knowledge can be used in the data fusion to create the air picture. However, passive radar systems rely on transmitters of opportunity, such as radio or television broadcast stations, which are not naturally designed for surveillance purposes. This leads to consequences in the data association.

2.1 Bistatic Pseudomaneuvers

Due to the bistatic geometry, even moderate Cartesian maneuvers can lead to quite sharp maneuvers in the bistatic measurement space. This is demonstrated in Figure 5: The left part shows the scenario configuration with one target moving along the black line, the (black) receiver in position [0,0] and three transmitters. After a straight flight, the target performs a turn to the right with 0.2 g and ends in straight flight again. In the Range-RangeRate-Space, this simple 3D-maneuver results in the three curves for the three different transmitters (Figure 5, right). Note especially the sharp turns for the blue and green illuminators. Stage 1 of the tracking algorithm should be capable of handling such maneuvers. In Cartesian space, natural maneuvers comprise smooth movements which can be covered by a mixture of different constant velocity or constant acceleration models. Transferred to Range-RangeRate-space, these movements do not inherit the natural and smooth behavior which we are used to in 3D-space and are more complicated to be modeled reasonably.

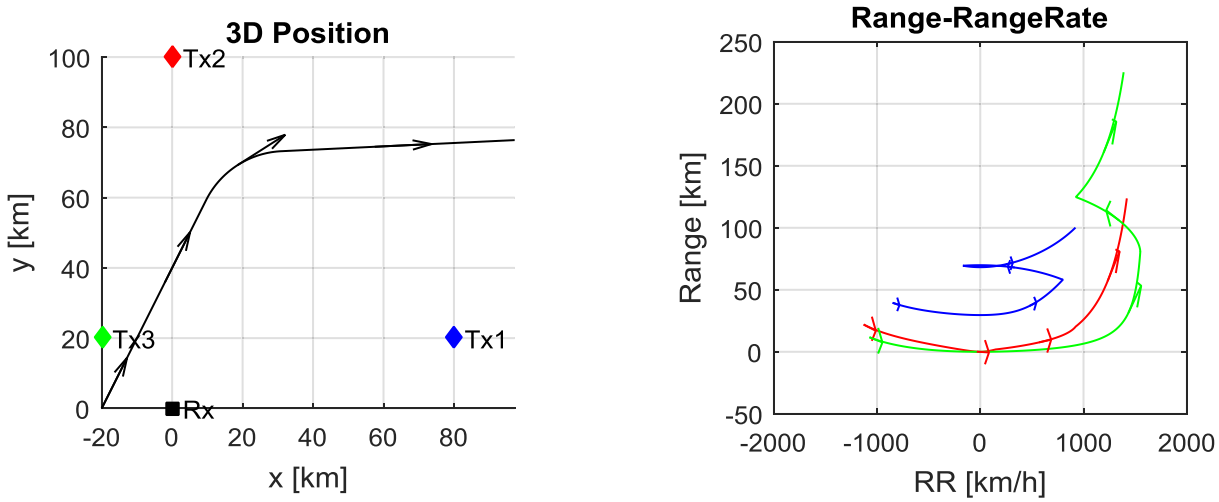

Figure 5: Range RangeRate Pseudo-Maneuvers.

2.2 Single Frequency Networks

For FM signals, the transmitter of a frequency is unique and, therefore, the emitting antenna can be clearly identified. However, e.g. DVB-T operates in single frequency networks (SFN), i.e., one and the same signal is emmitted simultaneously (or nearly simultaneously) from several antennas with different geographical locations, i.e. from several transmitters with different positions. Under ideal conditions, the sensor receives *one target echo for each illuminator* in a single frequency network at one instant of time. Due to the same frequency of all the signals, the actual illuminator that caused a reflection is unknown. *For each sensor-illuminator-network,* this leads to *N detections for one target*, with N being the number of illuminators in the SFN. Figure 6 explains this situation for N=3. For each illuminator, the true echo is received. Due to the uncertain origin of illumination, three possible target detections must be considered for each sensor-

illuminator-pair: the true detection plus two "ghost detections". The true detection cannot be selected directly, it is only known that two of the three detections must be false ones. The occurrence of ghost detections is symbolized by three same-coloured ellipses in Figure 6 (left) for each sensor-illuminator-pair. The Figure shows that besides the intersection of the ellipses in the true target location, this ambiguity leads to many additional ellipse intersections - which are possible target locations in the data fusion. Note that from the data fusion point of view the true target location is unknown. The underlying multiple hypothesis algorithms try to detect ghost targets and to distinguish them from the true target location. The many intersections of the ellipses in Figure 6 imply why this is computationally very demanding. Figure 6 (right) shows the consequences of this ambiguity in the R^3-Tracking (Stage 1): When analyzing the bistatic data over time in Stage 2 of the tracking algorithm, for each sensor-illuminator-pair three R^3-Tracks must be analyzed in contrast to one for the FM case (c.f. Figure 5, right). These tracks are range-shifted copies of each other, due to different distances between the sensor and the three illuminators. Here, the data ambiguity, i.e., the existence of multiple copies, extensively increases the computational load when a 3D-location of the target is desired and the pairwise ellipse intersections are calculated. The number of potential pairs dramatically increases by the multiple shifted copies of the target echo. The data fusion algorithms have to separate the "true" signal from the "ghost" signals over time. Note, that negative bistatic ranges can occur in the SFN case. In a single frequency network, the antenna focuses to one "reference illuminator", which is not necessarily the closest one to the receiver. If for another transmitter the distance from transmitter to target to receiver is smaller than the direct path from the reference illuminator to the receiver, this echo is received before the direct signal of the reference illuminator. This leads to plots with negative bistatic ranges.

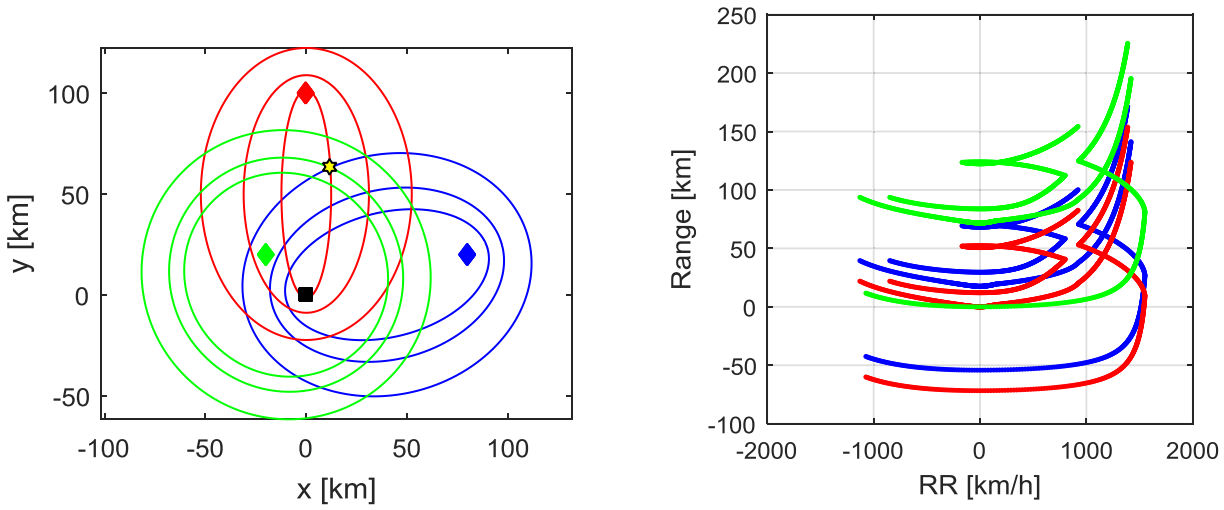

Figure 6: SFN Data (left: one instant of time, right: accumulated over time).

2.3 Non-Ideal Data

The effects described so far had the assumption of "ideal data", i.e., data from only one single target with a detection probability of 100% was assumed. Additional challenges occur when "real data" is investigated. The number of present targets is usually unknown. Especially in combination with the Cartesian incomplete nature of the measurements clutter or missing plots complicate the data association. As already mentioned in Section 1, measurement errors induce the need for more complicated mathematical tools from stochastics and numerics. Additionally all the effects presented so far were considered in 2D. Since the world is 3-dimensional and an altitude information is desired in the target reports, in fact (3-dimensional) ellipsoids instead of (2-dimensional) ellipses must be considered. An additional dimension complicates the mathematical equations and increases computational demand for their solutions considerably. To keep the

occurring mathematical problems in 2 dimensions, altitude hypothethes can be introduced. Instead of investigating the underlying 3D-problem, a set of 2D-problems can be extracted [7]. This way, the 3-dimensional world is cut into "slices" with different altitudes, solutions invoking the intersection of 2D-ellipses are calculated on these slices and afterwards combined again to 3D target reports.

3 REAL DATA

In this chapter we present measurement data and effects that occur in PR tracking. The underlying data was captured during a measurement campaign around Munich in 2015. Three PR receivers were involved which captured data from FM, DAB and DVB-T illuminators. All data was fused in a single PR tracking station.

3.1 Bistatic Plot Data

Figure 7 shows bistatic data (in Cartesian space) accumulated over 10 seconds. It has proven to be useful to plot not only the locations of the bistatic observations but also small ellipse segments which are defined by the locations of the illuminator and receiver, the bistatic range and azimuth. This way, intersections of several ellipses can be identified as target locations. The figure also visualizes with real data what was already shown in Figure 4: depending on the location geometry of sensor, illuminator and target the ellipse segments, which originate from the azimuth uncertainty, appear smaller or larger.

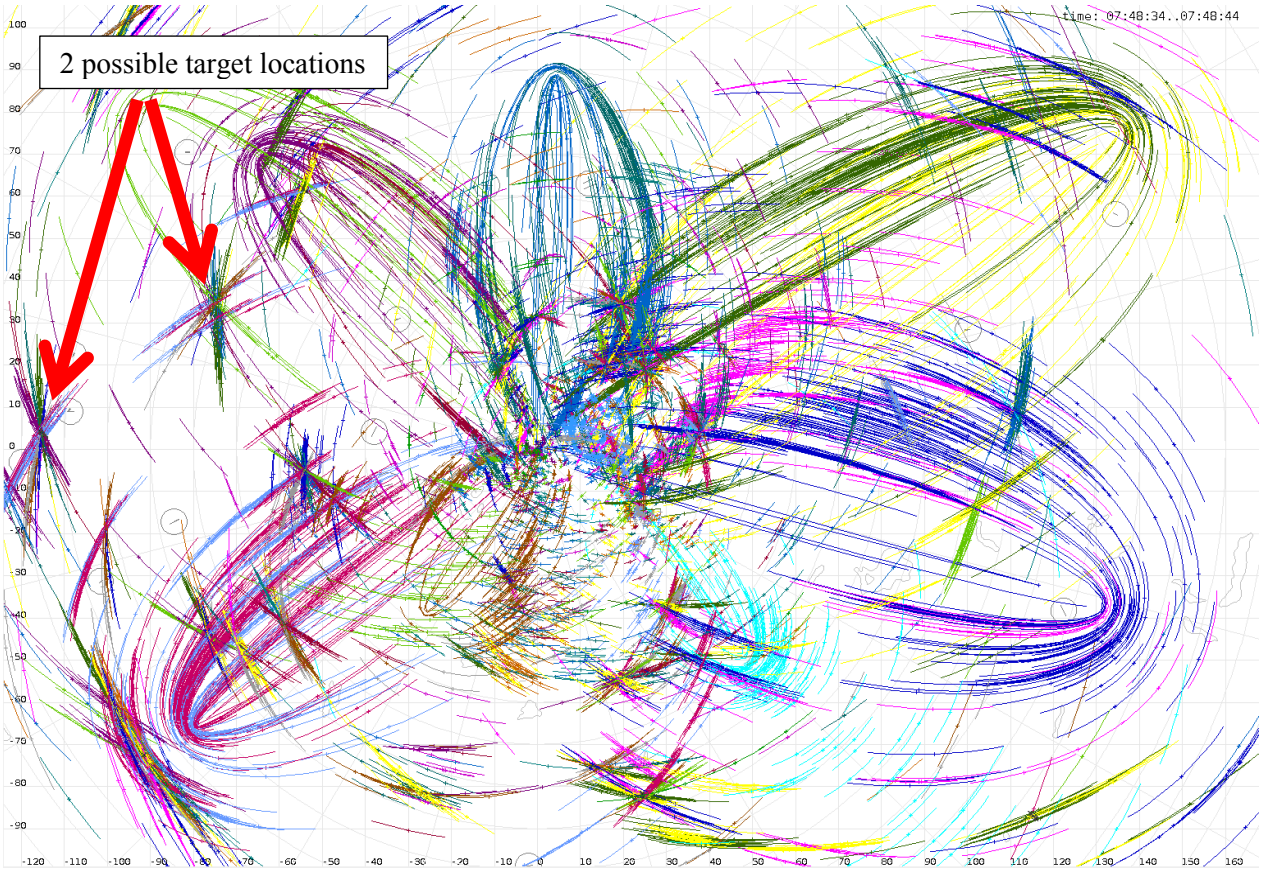

Figure 7: Bistatic Data.

3.2 R-RR-Space

In Figure 8, the received data in Range-RangeRate-Space accumulated over 30 seconds is shown. Stage 1 of the tracking algorithm is performed in this space (cf. Chapter 1.2). Traces can be identified and also the sharp (pseudo)maneuvers mentioned in Chapter 2.1 can be recognized.

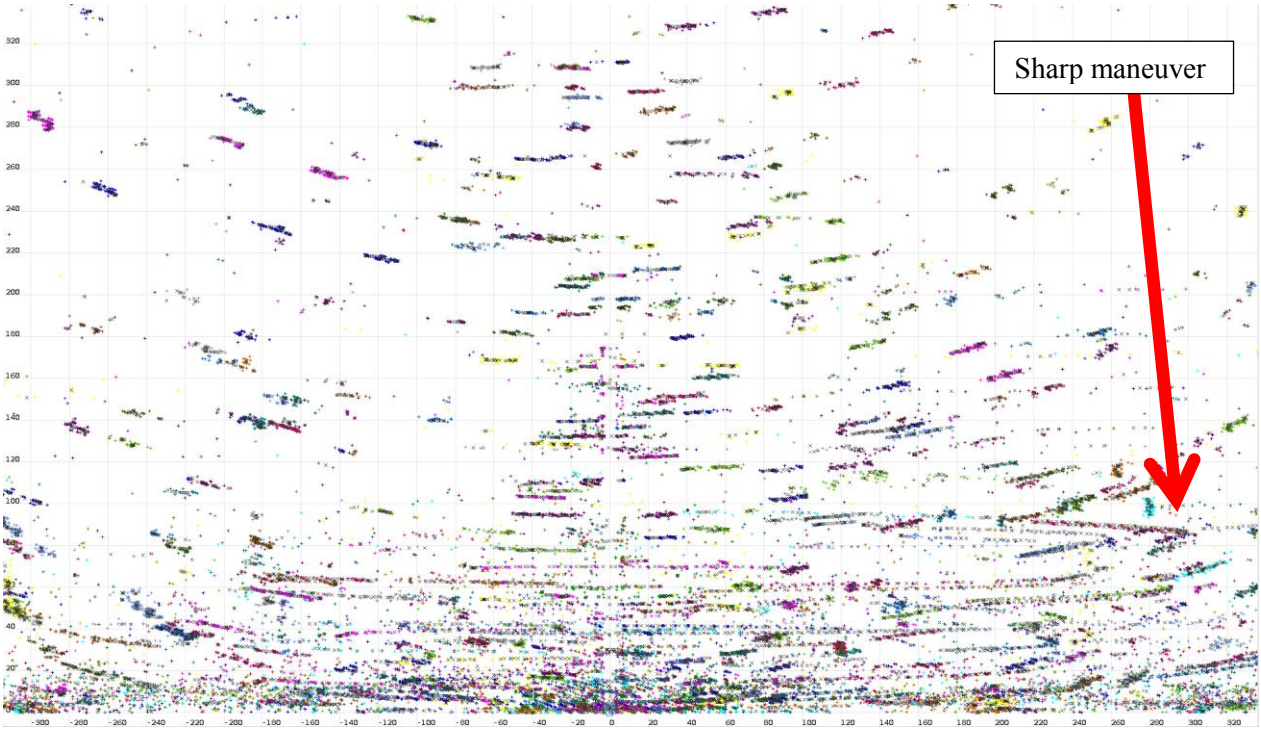

Figure 8: Range(y)-RangeRate(x)-Space.

3.3 Generation of 3D-Tracks

As a consequence of the 3-Stage-Tracking algorithm described in Chapter 1.2, one typical effect occurs when targets are detected for the first time, e.g. after take-off. This effect is visualized in Figure 9: First, R^3-Tracks (black) are initiated (a). When there are enough of them, they can be fused to 3D-Tracks (red) (b+c). Because of the feedback loop, bistatic plots are then directly associated to 3D-Tracks instead of R^3-Tracks. Since the R^3-Tracks are no longer supported by bistatic measurements, they are dropped whereas the 3D-Tracks are stabilized (c+d).

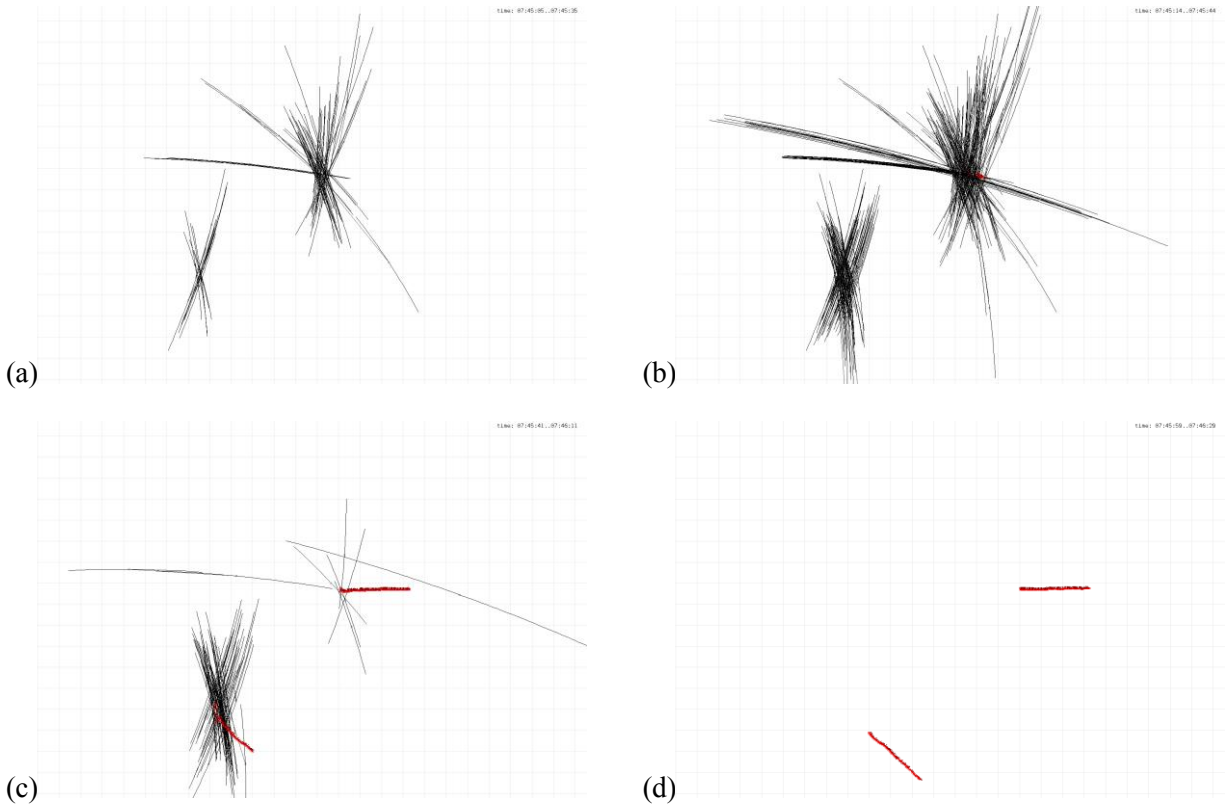

Figure 9: Generation of 3D-Tracks.

3.4 Air Situation Picture

Figure 10 shows the air situation picture accumulated over 120 seconds. 3D-Tracks generated by the passive radar cluster are shown in black, ADSB reference data is shown in green. Generally, the ADSB-targets are well-captured. In the lower left corner there are three targets without a 3D-Track, additionally there exist 3D-tracks without an ADSB-reference. The accuracy of the tracks can be improved further in some cases. These are ongoing tasks that are under recent investigation.

Figure 10: Air Situation Picture.

4 CONCLUSIONS

In this paper an overview of the principles of passive radar tracking is presented. The effects are shown in pictures rather than in complicated mathematics and formulas. The basic architecture of the tracking algorithm is described. Challenges occurring from the Cartesian-incomplete nature of the bistatic data and additional complications for the data association in single frequency networks are mentioned. After the theoretical considerations, results from real world data are presented.

5 ACKNOWLEDGMENT

The authors wish to thank Dr. Michael Wiedmann for many inputs to this work and for many valuable discussions.

6 REFERENCES

[1] Cherniakov, M, "Bistatic Radar: Principle and Practice", Wiley, 2007.

[2] Willis, N.J., Griffiths, H.D., "Advances in Bistatic Radar", SciTech Publishing, 2007.

[3] Edrich, M., Kloeck, C., Stroth, S. "A Passive Radar System for Long Range Air Surveillance", SET-241 9th NATO Military Sensing Symposium, Quebec, 2017.

[4] Malanowski, M., Kulpa, K., "Two Methods for Target Localization in Multistatic Passive Radar", IEEE Transactions on Aerospace and Electronic Systems, 2012.

[5] Wiedmann, M., Deininger, R., Schröder, A., Zimmermann, R., „Multi Transmitter Fusion for Tracking in a Network of Transmitters of Opportunity", SET-169-41 Symposium on 8th NATO Military Sensing Symposium, Friedrichshafen, 2011.

[6] Daun, M., Koch, W. "Multistatic Target Tracking for Non-Cooperative Illumination by DAB/DVB-T", IEEE Radar Conference, Rome, 2008.

[7] Daun, M., Kaune, R. "Gaussian Mixture Initialization in Passive Tracking Applications", 13th Conference on Information Fusion (FUSION), Edinburgh, 2010.